

Entanglement renormalization and topological order

Miguel Aguado

Max-Planck-Institut für Quantenoptik. Hans-Kopfermann-Str. 1. D-85748 Garching, Germany

Guifré Vidal

School of Physical Sciences. The University of Queensland. Brisbane, QLD, 4072, Australia

(Dated: February 11, 2013)

The multi-scale entanglement renormalisation ansatz (MERA) is argued to provide a natural description for topological states of matter. The case of Kitaev's toric code is analyzed in detail and shown to possess a remarkably simple MERA description leading to distillation of the topological degrees of freedom at the top of the tensor network. Kitaev states on an infinite lattice are also shown to be a fixed point of the RG flow associated with entanglement renormalization. All these results generalize to arbitrary quantum double models.

PACS numbers: 05.30.-d, 02.70.-c, 03.67.Mn, 05.50.+q

Renormalization group (RG) transformations aim to obtain an effective description of the large distance behavior of extended systems [1]. In the case of a system defined on a lattice, this can be achieved by constructing a sequence of increasingly coarse-grained lattices $\{\mathcal{L}_0, \mathcal{L}_1, \mathcal{L}_2, \dots\}$, where a single site of lattice \mathcal{L}_τ effectively describes a block of an increasingly large number $n_\tau \sim \exp(\tau)$ of sites in the original lattice \mathcal{L}_0 [2]. Real-space RG methods can, in particular, be applied to study quantum systems at zero temperature, in which case each site of \mathcal{L}_τ is represented by a Hilbert space \mathcal{K}_τ [3]. There the goal is to identify the local degrees of freedom relevant to the physics of the ground state and to retain them in the Hilbert space \mathcal{K}_τ , whose dimension d_τ must be large enough to describe this physics. A severe problem of such approach is that in $D \geq 2$ dimensions, d_τ must grow (doubly) exponentially in τ [4] as a result of the accumulation of short-range entanglement at the boundary of the block.

Entanglement renormalization [5] is a novel real-space RG transformation recently proposed in order to solve the above difficulties. Its defining feature is the use of *disentanglers* prior to the coarse-graining step. These are unitary operations, acting on the interface of the blocks defined by the RG procedure, that reduce the amount of entanglement in the system, see figure 1. A major achievement of the approach is that, when applied to a large class of ground states in both one [5] and two [6] spatial dimensions, the dimension d_τ is seen not to grow with τ . A steady d_τ is made possible by the disentangling step and has several implications [5, 6]. It means that, in principle, the resulting RG transformation can be iterated indefinitely at a constant computational cost, allowing for the exploration of arbitrarily large length scales. In addition, the system can be compared with itself at different length scales, and thus we can study RG flows in the space of ground state or Hamiltonian couplings. Finally, a constant d_τ also leads to an efficient representation of the system's ground state in terms of a tensor network, the *multi-scale entanglement renormalization ansatz* (MERA) [7].

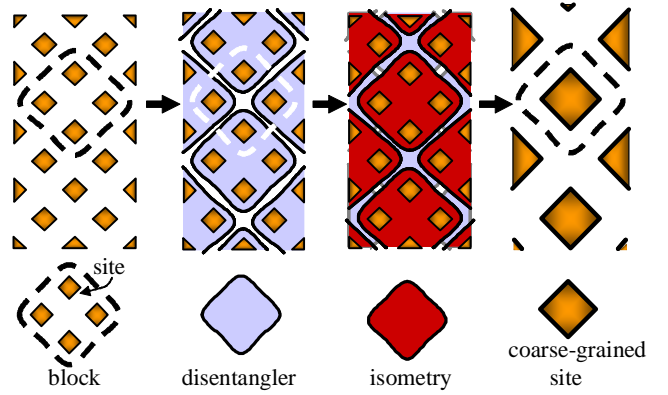


FIG. 1: RG transformation based on entanglement renormalization. In order to build an effective site from a block of four sites, we first apply disentanglers between sites of the block and surrounding sites. In this way part of the short-ranged entanglement between the block and its surroundings is removed. Then we coarse-grain the four sites into one by means of an isometry that selects the subspace $\mathcal{K}' \subseteq \mathcal{K}^{\otimes 4}$ to be kept. We show the case of a tilted square lattice in preparation for the toric code where, in addition, each site will contain four qubits.

At zero temperature, strongly correlated quantum systems appear organized in a plethora of *phases* or *orders*, including *local symmetry breaking* orders and *topological* orders [8]. Local symmetry breaking phases are described by a symmetry group and a local order parameter, and they are associated with the physical mechanism of condensation of point-like objects. Transitions between two such phases or orders involve a change in the symmetry, as described by Landau's theory. A simple picture emerges from the perspective of entanglement renormalization [5, 6]: under successive iterations of the RG transformation, ground states with local symmetry breaking order progressively lose their entanglement and eventually converge to a trivial fixed point, namely an unentangled ground state. On the other hand, critical ground states describing transitions between these phases

are non-trivial —that is, entangled— fixed points of the RG transformation. In either case, the MERA provides an efficient, accurate representation of the ground state.

Topological phases are fundamentally different from local symmetry breaking phases [8]. They do not stem from (the breakdown of) local group symmetries, but their *topological order* is linked to more complex mathematical objects, like tensor categories, topological quantum field theory, and quantum groups. Physically, topological phases exhibit gapped ground levels with robust degeneracy dependent only on the topology of the underlying space. This, and the fact that excitations above the ground level possess anyonic statistics, boosts the interest of these phases as scenarios for topological quantum information storage and processing. Condensation of string-like objects (in the so-called string-net models, see [9]) has been proposed as a general mechanism controlling topological phases. As may be expected, such profound differences are also reflected in the way the ground state is entangled. Specifically, the notion of topological entanglement entropy [10] (the subleading term in a large-perimeter expansion of the entanglement entropy of a system) has arisen as a quantitative measure of the ground state entanglement due to topological effects. Systems with topological order thus provide an unexplored scenario for entanglement renormalization techniques.

The purpose of this Letter is to establish entanglement renormalization and the MERA as valid tools also for the description and investigation of topological phases of matter. For simplicity, we analyze in detail Kitaev's toric code [11], a four-fold degenerate ground state widely discussed in the context of quantum computation and closely related to \mathbb{Z}_2 lattice gauge theory [12] and to the simplest of Levin-Wen's models for string-net condensation [9]. We show the following: (i) a MERA with finite, constant d_τ can represent the toric code *exactly*; (ii) at each iteration of the RG transformation, entanglement renormalization factors out local degrees of freedom from the lattice, while leaving the topological degrees of freedom untouched; (iii) the MERA representation of the four ground states is identical except in its top tensor, which stores the topological degrees of freedom; and (iv) in an infinite system, the toric code is the fixed point of this RG transformation. All these results also hold for more complicated models, such as quantum double lattice models, that we discuss in the appendix. We conclude that the MERA is naturally fitted to represent states with topological order, and the entanglement renormalization offers a new, useful framework for further studies.

Following [11], we consider a square lattice Λ on the torus, with spin-1/2 (qubit) degrees of freedom attached to each link. The Hamiltonian

$$H = - \sum_+ A_+ - \sum_{\square} B_{\square} \quad (1)$$

is a sum of constraint operators associated with vertices

‘+’ and plaquettes ‘ \square ,’ namely

$$A_+ = \prod_{i \in +} X_i, \quad B_{\square} = \prod_{i \in \square} Z_i. \quad (2)$$

Stabilizers A_+ act as a simultaneous spin flip in all four qubits adjacent to a given vertex. Stabilizers B_{\square} yield the product of group assignments ± 1 at the four qubits around a plaquette. All stabilizers commute with each other and have eigenvalues ± 1 . Hamiltonian (1) is gapped, and states in the ground level (Kitaev states) are simultaneous eigenstates of all A_+ , B_{\square} with eigenvalue +1. The degeneracy of the ground level (i.e., the number of Kitaev states) depends on the topology of the manifold underlying the lattice. If this manifold is a topologically nontrivial Riemann surface, information is encoded in nontrivial cycles, since operators $\prod_{i \in \mathcal{C}_{a,b}} Z_i$, where $\mathcal{C}_{a,b}$ are nontrivial cycles along bonds of the lattice, commute with all stabilizers. Besides, such operators along homologically equivalent nontrivial cycles $\mathcal{C}_a, \tilde{\mathcal{C}}_a$ have the same action on Kitaev states. Hence, for a torus, two logical qubits are encoded in the action of these operators.

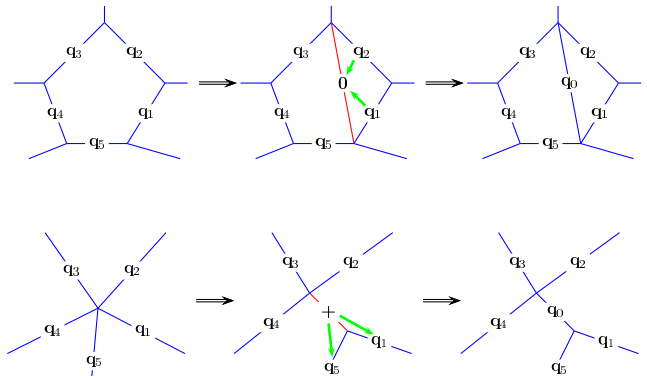


FIG. 2: Elementary moves adding plaquettes and vertices to a toric code. Arrows stand for CNOT operations.

Kitaev states are efficiently written in terms of their stabilizers. The stabilizer formalism [13] also provides us with a useful language to analyse the action of operators on Kitaev states, and has proved instrumental in finding an exact MERA. The key observation to this purpose is that there exist ‘elementary moves’ [14], minimal deformations of the lattice and its Kitaev states, that respect the topological characteristics of the code. These moves consist of addition or removal of faces and vertices together with qubits, and can be written in terms of controlled-NOT (CNOT) operators, whose adjoint action has a very simple expression in terms of stabilizers:

$$I \otimes Z \leftrightarrow Z \otimes Z, \quad Z \otimes I \mapsto Z \otimes I, \quad (3)$$

$$I \otimes X \mapsto I \otimes X, \quad X \otimes I \leftrightarrow X \otimes X. \quad (4)$$

Figure 2 depicts the construction of elementary moves. The creation of a face is achieved by introducing a new spin in a plaquette. Arrows stand for CNOT operators from control qubits (all qubits in one of the semiplaquettes) to the target qubit (the new qubit, introduced in

state $|0\rangle$). The following transformation of stabilizers holds (the new site is denoted as n):

$$Z_1 Z_2 Z_3 Z_4 Z_5 \mapsto Z_1 Z_2 Z_3 Z_4 Z_5, \quad (5)$$

$$Z_n \mapsto Z_1 Z_2 Z_n, \quad (6)$$

which ensures plaquette constraints are obeyed. Similarly, the two relevant vertex constraints are extended to the new qubit. The creation of a new vertex is achieved instead by introducing a new qubit in state $|+\rangle$. This qubit now plays the role of control for CNOTs acting on the qubits adjacent to one of the split vertices. Stabilizers transform as

$$X_1 X_2 X_3 X_4 X_5 \mapsto X_1 X_2 X_3 X_4 X_5, \quad (7)$$

$$X_n \mapsto X_5 X_1 X_n, \quad (8)$$

which is again compatible with the code constraints. Both final sets of operators are the correct stabilizers for the code in the modified lattice (remember that $X^2 = Z^2 = I$.) Similarly, the two relevant plaquette constraints are extended to the new qubit.

These operations can be inverted to *decouple* qubits in states $|0\rangle$ and $|+\rangle$ from the rest system. The disentanglers and isometries, defining both the RG transformation and the MERA for the Kitaev states, are made of several of these decoupling moves. We regard the original square lattice Λ , on which the toric code is defined, as a (tilted) square lattice \mathcal{L}_0 where each site contains four qubits. Then both disentanglers and isometries act on blocks of four sites of \mathcal{L}_0 as in figure 1 — equivalently, on blocks of 16 qubits in Λ . They consist of a series of CNOTs as specified in figures 3 and 4.

Upon applying the RG transformation, we obtain a coarse-grained lattice \mathcal{L}_1 which is locally identical to \mathcal{L}_0 and where, by construction, the toric code constraints are still satisfied. This is quite remarkable. On the one hand, it is the first non-trivial example, in the context of entanglement renormalization, where the RG transformation is *exact* [15], leading to the first non-trivial model that can be *exactly* described with the MERA. On the other hand, if we consider an infinite lattice, the above observation implies that Kitaev states are an explicit fixed point of the RG flow in the space of ground states, as induced by the present RG transformation [16].

Let us now consider a finite lattice \mathcal{L}_0 on the torus. The coarse-grained state carries exactly the same topological information (values of $\prod Z$ along nontrivial cycles) as the original state, since the elementary moves preserve such information at each intermediate step. That is, different Kitaev states are not mixed during the RG transformation. By iteration, we obtain a sequence of increasingly coarse-grained lattices $\{\mathcal{L}_0, \mathcal{L}_1, \mathcal{L}_2, \dots, \mathcal{L}_T\}$ for ever smaller toruses. The top lattice \mathcal{L}_T will contain only a few qubits. Recall that the MERA is made of all the disentanglers and isometries used in the RG transformations, together with a top tensor describing the state of \mathcal{L}_T [7]. It follows that the MERAs for different states of the toric code will contain identical disentanglers and

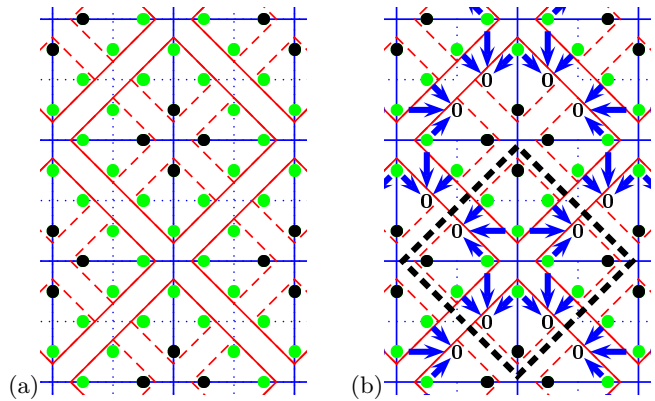


FIG. 3: (a) The square lattice Λ for the toric code, with qubits (dots) on the links, is reorganized into a tilted square lattice \mathcal{L}_0 where each site is made of four qubits. The lattice constant is doubled (dotted lines disappear) after the RG transformation, which produces a new four-qubit site for lattice \mathcal{L}_1 from every block of sixteen qubits (the twelve light qubits in the block are decoupled in known product states). (b) First step of the RG transformation: Disentanglers. Arrows stand for simultaneous CNOT operators from control to target qubits. Disentanglers act on sixteen-qubit domains overlapping with four blocks each (thick dashed line, cf. figure 1.) Four qubits per block decouple in state $|0\rangle$.

isometries, and will only differ in their top tensor, where all the topological information is stored.

All the above results automatically extend to the loop model considered by Levin and Wen as the simplest of their family of string-net models [9]. Indeed, the toric code on a square lattice can be locally transformed, using the decoupling moves depicted in figure 5, into a toric code on a triangular lattice, which is equivalent to the ground state of the loop model defined on the dual (hexagonal) lattice. This local transformation shows that the topological order of both models are identical, a fact already pointed out in [17] and which can also be understood in terms of the projected entangled-pair state ansatz (PEPS) [18].

Finally, our construction generalizes almost straightforwardly to quantum double models (see, e.g., [11]), both for Abelian and non-Abelian groups. This is achieved by replacing CNOTs with controlled group multiplication operators and by paying due attention to the order of the operations (see appendix).

In conclusion, we have shown that several models with topological order can be exactly represented with the MERA, where topological degrees of freedom are naturally isolated in its top tensor. We have also seen that such models are fixed points of the RG flow induced by entanglement renormalization. Our results are an unambiguous sign that entanglement renormalization and the MERA, originally developed to efficiently simulate systems with local symmetry-breaking phases, provide also a most natural framework to study topological phases.

Acknowledgements: We thank J. I. Cirac, A. Ki-

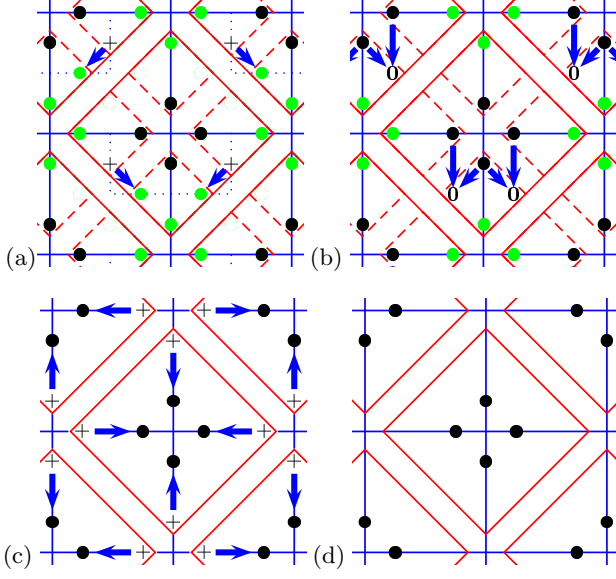


FIG. 4: (a)–(c) Second step of the RG transformation: Isometries. (a) Two qubits per block decouple in state $|+\rangle$. (b) Two more qubits per block decouple in state $|0\rangle$. (c) One qubit per edge, four per block, decouple in state $|+\rangle$. The isometry also traces out the twelve decoupled qubits. (d) State of the system after the RG transformation.

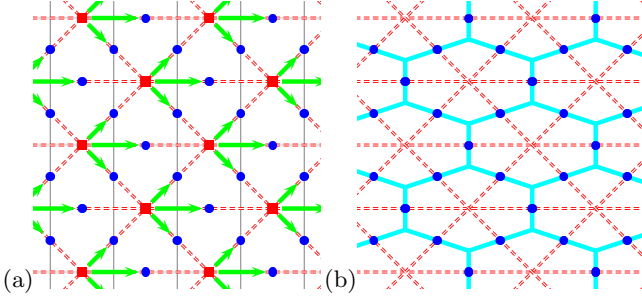


FIG. 5: Local mapping between the toric code on a square lattice (a) and on a triangular lattice (b). The dual model in a honeycomb lattice (displayed for reference) is Levin and Wen's loop model.

taev, D. Pérez-García, J. Preskill and F. Verstraete for related discussions. M. A. thanks the University of Queensland for hospitality and a stimulating working atmosphere during his visit. G. V. acknowledges financial support from the Australian Research Council, FF0668731.

APPENDIX A: EXACT MERA FOR QUANTUM DOUBLE MODELS

Here we generalize the above RG transformation and MERA to lattice quantum double models (see [11].) Local degrees of freedom are associated with *oriented* bonds of a lattice Λ and identified with the group algebra of a discrete, in general non-Abelian, group G , i.e., the Hilbert space spanned by an orthonormal ba-

sis $\{|g\rangle, g \in G\}$. A change in the orientation of a bond corresponds to the map $S : |g\rangle \mapsto |g^{-1}\rangle$. The Hamiltonian is a sum of mutually commuting projectors over vertices and plaquettes,

$$H_{D(G)} = - \sum_v A_v - \sum_p B_p \quad (\text{A1})$$

where vertex projector A_v acts on edges incoming to vertex v by simultaneous right multiplication by each group element,

$$A_v = \frac{1}{|G|} \sum_{h \in G} \bigotimes_{i \rightarrow v} R_i(h), \quad (\text{A2})$$

right multiplication acts as $R(h)|g\rangle = |gh\rangle$, and plaquette projector B_p selects configurations where the ordered product of group elements taken along an oriented circuit \mathcal{C}_p around p is the unit element of G ,

$$B_p = \delta\left(\prod_{i \text{ along } \mathcal{C}_p} g_i, e\right). \quad (\text{A3})$$

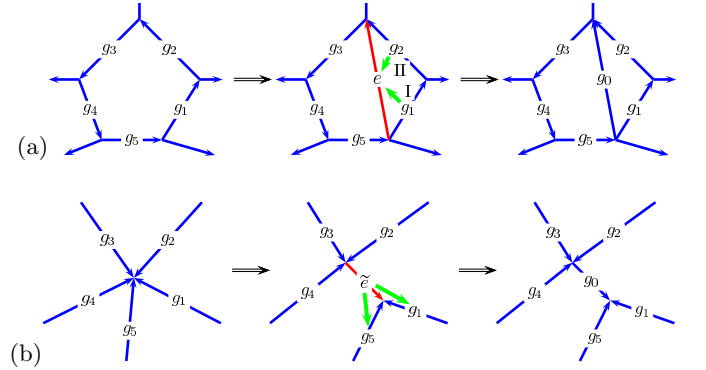


FIG. 6: Elementary moves adding plaquettes and vertices to a quantum double model. Local degrees of freedom live in the group algebra of a discrete group G . The ancilla is initialised in state $|e\rangle$ (unit element of G). Thick arrows stand for controlled right-multiplication of the target element by the control element. Orientation of the edges plays an important rôle. (a) For plaquette addition, operations must be performed in a prescribed order (e.g., after application of the arrows in counterclockwise order (I, II), the new element becomes $g_1 g_2$.) (b) For vertex addition, the new element is initialised in state $|\tilde{e}\rangle$, the equal-weight superposition of all elements in G . Here all operations can be performed simultaneously.

Elementary moves are analogous to their counterparts for the toric code. The operations generalising CNOTs are controlled multiplications by the control element (CMs). Figure 6 shows how to create plaquettes and vertices using the controlled right multiplication

$$A|h, g\rangle = |h, gh\rangle, \quad (\text{A4})$$

where the first element is the control and the second element is the target. To cover the case of different bond orientations, we also consider the transformations

$B = (S \otimes 1)A(S \otimes 1)$, $C = (1 \otimes S)A(1 \otimes S)$, and $D = (S \otimes S)A(S \otimes S)$; explicitly:

$$\begin{aligned} B|h, g\rangle &= |h, gh^{-1}\rangle, \\ C|h, g\rangle &= |h, h^{-1}g\rangle, \\ D|h, g\rangle &= |h, hg\rangle. \end{aligned} \quad (\text{A5})$$

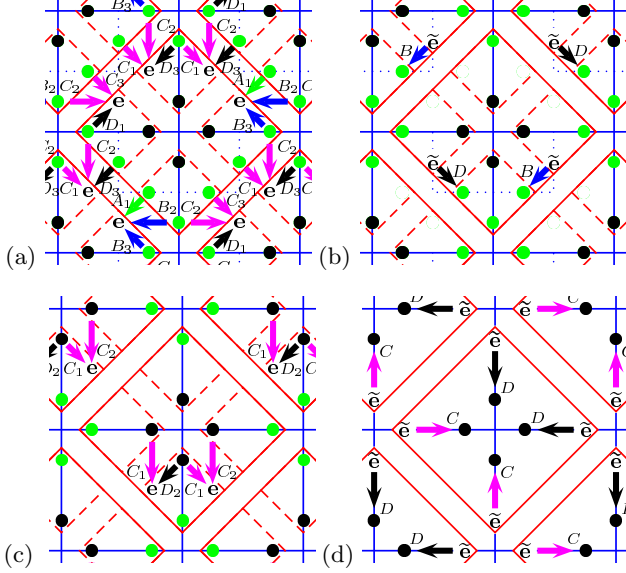


FIG. 7: RG transformation for a quantum double model. Arrows stand for controlled multiplications (CM) from control to target elements. Arrow labels denote the type of CM (see equations (A4) and (A5)), as well as the order in which they are applied within each step. The fiducial lattice orientation (horizontal bonds pointing to the right, vertical bonds pointing upwards) is assumed. (a) Disentangler. Four elements per block decouple in state $|e\rangle$. (b)–(c) Isometries. In (b), two elements per block decouple in state $|\tilde{e}\rangle$. In (c), another two elements per block decouple in state $|e\rangle$, and the lattice becomes a doubled square lattice with two elements per edge. One element per edge, four per block, then decouple in (d) in state $|\tilde{e}\rangle$, completing the MERA ansatz.

By means of these operations, new edges initialised in states $|\tilde{e}\rangle$ and

$$|\tilde{e}\rangle = \frac{1}{\sqrt{|G|}} \sum_{h \in G} |h\rangle \quad (\text{A6})$$

are incorporated into the code, creating new plaquettes and vertices. Of course, the inverse elementary moves *removing* plaquettes and vertices from the code, needed for the MERA construction, are in general not identical to those adding plaquettes and vertices. Note that operations leading to plaquette addition (or removal) cannot be performed simultaneously for non-Abelian groups, since the order of multiplication of the elements is important.

The RG transformation corresponding to a quantum double model associated with group G and defined on a square lattice proceeds along the same lines as for the toric code, but there are qualitative differences. To fix the setting, we work with a fiducial orientation of the bonds: horizontal bonds are oriented from left to right and vertical bonds are oriented upwards. Then:

- Operations within a plaquette cannot be performed simultaneously and must be applied in a certain order. Hence, disentanglers must be applied in three steps, while isometries demand another step with respect to the toric code RG.
- Which of the controlled operations A, B, C, D is needed at each step depends on the bond orientations.

The explicit form of the RG leading to a MERA description of the quantum double model is shown in figure 7. The basic properties of the toric code MERA (bounded causal cone, topological degrees of freedom at the top of the tensor network, ER fixed point in the infinite lattice limit) generalise to the quantum double setting.

[1] M. E. Fisher, Rev. Mod. Phys. **70**, 653 (1998).
[2] L. P. Kadanoff, Physics **2**, 263 (1966).
[3] K. G. Wilson, Rev. Mod. Phys. **47**, 773–840 (1975).
S. R. White, Phys. Rev. Lett. **69**, 2863 (1992),
Phys. Rev. **B48**, 10345 (1993).
[4] In a D dimensional lattice the ground state typically obeys a boundary law $S_l \sim l^{D-1}$ for the entanglement entropy of a block of l^D sites. In this case the dimension d_τ for a site of \mathcal{L}_τ must at least scale doubly exponentially in τ , $d_\tau \sim \exp(\exp(\tau))$. Indeed, on the one hand the dimension of an effective space for a block of l^D sites must be at least $d \sim \exp(S_l) = \exp(l^{D-1})$. On the other, $l_\tau \sim \exp(\tau)$ after τ iterations of the RG transformation, where $n_\tau = l_\tau^D$ is the number of sites of \mathcal{L}_0 effectively described by a single site of \mathcal{L}_τ .
[5] G. Vidal, Phys. Rev. Lett. **99**, 220405 (2007), arXiv:

cond-mat/0512165v2 [cond-mat.str-el].
[6] G. Evenbly, G. Vidal, arXiv:0710.0692v2 [quant-ph];
G. Evenbly, G. Vidal, arXiv:0801.2449v2 [quant-ph].
[7] G. Vidal, arXiv:quant-ph/0610099.
[8] X.-G. Wen, *Quantum Field Theory of Many-Body Systems*, Oxford University Press (2004).
[9] M. A. Levin, X.-G. Wen, Phys. Rev. **B71** 045110 (2005),
arXiv:cond-mat/0404617v2 [cond-mat.str-el].
[10] A. Hamma, R. Ionicioiu, P. Zanardi, Phys. Rev. **A71**,
022315 (2005), arXiv:quant-ph/0409073v2. A. Kitaev,
J. Preskill, Phys. Rev. Lett. **96**, 110404 (2006),
arXiv:hep-th/0510092v2. M. Levin, X.-G. Wen, Phys.
Rev. Lett. **96**, 110405 (2006), arXiv:cond-mat/0510613v2
[cond-mat.str-el].
[11] A. Yu. Kitaev, Annals Phys. **303**, 2–30 (2003), arXiv:
quant-ph/9707021v1.

- [12] F. J. Wegner, J. Math. Phys. **12**, 2259–2272 (1971).
- [13] D. Gottesman, Ph.D. thesis, Caltech, 1997, [arXiv:quant-ph/9705052v1](#).
- [14] E. Dennis et al., J. Math. Phys. **43**, 4452–4505 (2002), [arXiv:quant-ph/0110143v1](#).
- [15] Notice that the qubits being removed from the lattice during the RG transformation are *exactly* in a product state. In all previous examples [5, 6] it was only possible to *approximately* disentangle the subsystems before their removal.
- [16] This points to a more general result, to be discussed elsewhere: under the present RG transformation based on entanglement renormalization, systems with topological order flow toward the string-net models of Levin and Wen [9], substantiating ideas already advocated by these authors.
- [17] Z. Nussinov, G. Ortiz, [arXiv:cond-mat/0702377v5 \[cond-mat.str-el\]](#).
- [18] F. Verstraete, M. M. Wolf, D. Pérez-García, and J. I. Cirac, Phys. Rev. Lett. **96**, 220601 (2006), [arXiv:quant-ph/0601075v2](#).